





ORIGINAL RESEARCH ARTICLE

Open Access



The role of hepatic transcription factor cAMP response element-binding protein (CREB) during the development of experimental nonalcoholic fatty liver: a biochemical and histomorphometric study

Ashraf K. Awaad^{1,2,3*} , Maher A. Kamel², Magdy M. Mohamed¹, Madiha H. Helmy², Magda I. Youssef⁴, Eiman I. Zaki⁵, Marwa M. Essawy^{3,6}  and Marwa G. A. Hegazy¹

Abstract

Background: Several molecular mechanisms contribute to the initiation and progression of nonalcoholic fatty liver disease (NAFLD); however, the exact mechanism is not completely understood. Cyclic adenosine monophosphate (cAMP) is one of the most promising pathways that regulates various cellular functions including lipid and carbohydrate metabolism. cAMP induces gene transcription through phosphorylation of the transcription factor, cAMP response element-binding protein (CREB). The action of cAMP is tightly regulated by its level and repression. Among the repressors, Inducible cAMP Early Repressor (ICER) is the only inducible CRE-binding protein. The present study aimed to evaluate the role of hepatic CREB level in the development of experimental NAFLD model to clarify the pathogenesis of the disease. NAFLD 35 male Wistar rats fed a high fat diet for a period of 14 weeks were studied compared with 35 control rats fed a standard diet. Five fasting rats were sacrificed each 2 weeks intervals for a period of 14 weeks.

Results: NAFLD group revealed a remarkable duration—dependent elevation in cAMP and CREB levels in the liver tissue compared to control group (P value < 0.004, P value < 0.006, respectively). In contrast, ICER gene expression, as a dominant-negative regulator of CREB, was downregulated in the liver of NAFLD group compared to control group. We also demonstrated that CREB levels were positively correlated with liver function tests, and glucose homeostasis parameters.

Conclusions: Our results indicate that cAMP/CREB pathway provides an early signal in the progression to NAFLD representing a noninvasive biomarker that can early detect NAFLD and a promising therapeutic target for the treatment of the disease as well.

Keywords: Nonalcoholic fatty liver disease, Cyclic adenosine monophosphate, cAMP response element-binding protein, Inducible cAMP early repressor

* Correspondence: ashrafawaad24@gmail.com

¹Biochemistry Department, Faculty of Science, Ain Shams University, Cairo, Egypt

²Biochemistry Department, Medical Research Institute, Alexandria University, Alexandria, Egypt

Full list of author information is available at the end of the article



© The Author(s) 2020, corrected publication 2020. **Open Access** This article is licensed under a Creative Commons Attribution 4.0 International License, which permits use, sharing, adaptation, distribution and reproduction in any medium or format, as long as you give appropriate credit to the original author(s) and the source, provide a link to the Creative Commons licence, and indicate if changes were made. The images or other third party material in this article are included in the article's Creative Commons licence, unless indicated otherwise in a credit line to the material. If material is not included in the article's Creative Commons licence and your intended use is not permitted by statutory regulation or exceeds the permitted use, you will need to obtain permission directly from the copyright holder. To view a copy of this licence, visit <http://creativecommons.org/licenses/by/4.0/>.

Background

Nonalcoholic fatty liver disease (NAFLD) is currently the most prevalent chronic liver disease in developed countries because of the obesity epidemic. NAFLD widely ranges from asymptomatic hepatic steatosis to more advanced liver disease with hepatic failure or hepatocellular carcinoma [1, 2].

NAFLD is considered as a metabolic disorder that results from complex interaction between genetic, hormonal, and nutritional factors. Obesity and metabolic syndromes are the most important risk factors identified in the development and progression of NAFLD [3, 4].

The hallmark feature of NAFLD is steatohepatitis which occurs when the rate of hepatic fatty acid uptake from plasma and de novo fatty acid synthesis is greater than the rate of fatty acid oxidation and export as triglyceride within very low-density lipoprotein (VLDL). Therefore, an excessive amount of intrahepatic triglyceride represents an imbalance between complex interactions of metabolic events [5].

Adenylyl cyclase is a membrane-bound enzyme that catalyzes the conversion of ATP to cAMP. cAMP acts as a second messenger through activation of protein kinase A (PKA) by dissociating its regulatory subunit from the catalytic subunit [6]. The PKA phosphorylates and activates a wide range of proteins at serine and threonine residues including the transcription factor cAMP response element-binding protein (CREB) at Ser133, which leads to the nuclear localization CREB [7].

Intracellular levels of cAMP are tightly regulated by its activation as well as its repression. Inducible cAMP early repressor (ICER) is generated from an alternative cAMP response element-modulator (CREM) promoter and is the only inducible CRE-binding protein. The activity of the CREB factors is abundantly modulated by the level of ICER [8]. Indeed, ICER plays a dominant-negative role by competing with all cAMP-responsive transcriptional activators of the CREB and CREM and activating transcription factor families for binding to CRE. ICER is temporarily increased, after its generation, and immediately returns to its normal levels. Dysregulation in the expression of ICER leads to various metabolic defects [9].

In response to different metabolic conditions, hepatic lipid and carbohydrate homeostasis are tightly and coordinately regulated by nuclear receptors, transcription factors, and cellular enzymes [10, 11]. CREB widely plays important roles in hepatic lipogenesis, fatty acid oxidation, and lipolysis as well as glucose metabolism [12, 13]. The current study aimed to evaluate the role of hepatic CREB level in the development of experimental NAFLD to clarify the pathogenesis of the disease.

Methods

Experimental animals

Seventy male Wistar rats, weighed 100–120 g, were purchased from the Medical Technology Center, Alexandria University, Egypt. The rats were housed at a temperature of 23 ± 1 °C with 12/12 h light/dark cycles and $45 \pm 5\%$ humidity with free access to water and chow diet for a week prior to the experiment [14]. The rats were weighed at the beginning and at the end of the experiment. The study was approved by the Alexandria University Institutional Animal Care and Use Committee (ALEXU-IACUC; AU01220051022) for the animal experimentation.

Experimental design

Rats were randomly divided into two groups (35 each): control group which fed a standard diet and NAFLD group that fed a high fat diet (HFD) for 14 weeks. The HFD consisted of commercial rat chow plus peanuts, milk chocolate, and sweet biscuit in a proportion of 3:2:2:1. All components of the high-fat diet were ground and blended [15]. Five rats from each two groups were fasted overnight, weighed, anaesthetized with diethyl ether, and sacrificed by cervical dislocation each 2 weeks for a period of 14 weeks. The blood samples were collected for serum separation then stored at -80 °C, for biochemical analyses. The whole liver was immediately removed and weighed. One lobe from each animal was removed for histological assessment; the remaining lobes were stored at -80 °C, for cAMP and CREB quantification by ELSA kits and *ICER* gene expression level by reverse transcriptase polymerase chain reaction (RT-PCR).

Determination of liver function tests

The activities of alanine aminotransferase (ALT), aspartate aminotransferase (AST), and gamma glutamyl transferase (GGT) were measured using a commercial diagnostic kit (Randox Laboratories Ltd, Crumlin, UK) according to the manufacturer's protocol. Total and direct bilirubin levels were measured using a diagnostic kit (Spectrum Diagnostics Co., Cairo, Egypt) according to the manufacturer's protocol. All biochemical analysis and their absorbance were read using a spectrophotometer (Photometer 5010 V5+ RIELE GmbH & Co KG Berlin Germany).

Determination of serum lipid profile

Serum lipid profile including triglycerides (TG), total cholesterol (TC), high-density lipoprotein (HDL-C), and low-density lipoprotein (LDL-C) was assessed by using a commercial diagnostic kit (Randox Laboratory Ltd, Crumlin, UK) according to the manufacturer's instructions.

Determination of hepatic cholesterol and triglyceride content

Hepatic lipid contents were extracted and determined, according to Folch et al. [16]. Briefly, 500 mg of liver tissues was homogenized in 5 ml of a chloroform/methanol (2:1) mixture in ice bath. The extract was centrifuged for 15 min at 2500×g, and the supernatant was collected and evaporated to dryness under nitrogen. The residue was thereby reconstituted in a solution of isopropyl alcohol containing 10% Triton X and centrifuged for 10 min at 10,000×g. The supernatant was used for the detection of triglycerides and cholesterol content using a colorimetric diagnostic kit (Randox Laboratory Ltd, Crumlin, UK), according to the manufacturer's protocol.

Determination of serum glucose, insulin, and insulin resistance (IR)

The level of serum glucose was determined by using a commercial kit (Human diagnostics, Germany). Serum insulin level was quantified using a commercial ELISA kit (Millipore, Germany) according to the manufacturer's protocol. The insulin resistance index (IRI) was estimated by homeostasis model (HOMA-IR), where $IRI = [\text{fasting insulin } (\mu\text{U/ml}) \times \text{fasting glucose (mmol/l)}] / 22.5$ [17].

Determination of the hepatic cyclic AMP

The cyclic AMP direct ELISA Immunoassay kit (DRG International, Inc, Springfield, USA) is designed to quantitatively measure cAMP present in tissue samples according to Serezani et al. [18]. The level of cAMP was finally calculated in terms of protein content in each tissue sample measured by Lowry et al. [19].

Determination of the hepatic CREB

The total CREB kit (Invitrogen, Camarillo, CA, USA) is a solid phase sandwich Enzyme Linked-Immuno-Sorbent Assay (ELISA) which is designed to quantitatively measure total CREB present in tissue samples according to the manufacturer's protocol.

Determination of ICER gene expression

Total RNA was isolated from liver tissues using TRIzol RNA isolation kit (Invitrogen, Life Technologies, Carlsbad, CA, USA) according to the manufacturer's instructions. The yield of total RNA obtained was determined using a NanoDrop 2000 spectrophotometer (Thermo Fischer Scientific, USA). The absorbance of total RNA was measured at 260 nm and 280 nm. The purity of total RNA was determined by taking the ratio of A 260 and A 280. Quantitative RT-PCR was applied to determine the relative expression of *ICER*. The relative quantification (RQ) using comparative threshold cycle (Ct) provides an accurate comparison between the initial levels of template in each sample. A normalizer or reference gene

(glyceraldehyde 3-phosphate dehydrogenase "*GAPDH*") was used as internal control for experimental variability [20].

Quantitative RT-PCR assay was carried out using Rotor-Gene SYBR Green RT-PCR Kit (Qiagen, Valencia, CA, USA). The PCR primer sequences used in gene expression analysis are provided in Table 1. The expected unique amplification of *ICER* and *GAPDH* genes is confirmed by blasting pairs of primer sequences against NCBI/Primer Blast. The analyses were performed as duplicates. QIAGEN's real-time PCR cycler, the Rotor-Gene Q (Qiagen, Valencia, CA, USA), was used.

Histological assessment and determination of phosphorylated CREB (phospho S133) by immunofluorescence

Liver specimens were excised and fixed in 10% buffered formalin. They were processed for hematoxylin and eosin (H&E) stain for histological assessment [23, 24]. Digital images from liver sections were taken using a digital camera (Olympus DP20) joined to microscope (Olympus BX41). Images were captured at magnification × 100 and × 400, to determine histological alterations.

Immunofluorescence staining was performed according to the protocols described by Bártová et al. [25]. Briefly, sections were permeabilized with Triton X 0.1% for 10 min at room temperature. The slides were washed twice with PBS for 5 min each time. Non-specific staining was blocked by incubation with bovine serum albumin 1% for 45 min at room temperature; the slides were then washed twice with PBS for 5 min each time. The sections were incubated with Anti-CREB (Ser133, cat. no. ab32096; Abcam, Cambridge, UK) antibody, according to the manufacturer's instructions, overnight at 4 °C in a humidified chamber. At the next day, sections were washed three times with PBS for 5 min each time. The tissues were then incubated with goat anti-rabbit Alexa Fluor 594 secondary antibody (#A11012, Invitrogen, USA) at room temperature for 1 h in the dark. After incubation, the sections were washed three times with PBS for 5 min, followed by DNA counterstaining with DAPI (4',6-diamidino-2-phenylindole) (Sigma-Aldrich, branch in the Czech Republic) dissolved in the mounting medium Vectashield (Vector Laboratories, USA). The specific staining was visualized, and images were acquired using confocal laser scanning microscopy (Leica TSC SPE II/DMi 8). The photomicrographs were morphometric analyzed in terms of mean area percent (MA%) and intensity of fluorescence using an image analysis software (Image J; 1.52p software 32, NIH, USA).

Statistical analysis

Statistical analysis was performed using the SPSS version 18 software. All data obtained were presented as mean ±

Table 1 Gene nomenclature, GenBank accession code, and primer sequences for *Mus musculus* (house mouse) gene expression analysis with qRT-PCR

Gene	The reference sequence	Forward (F) and reverse (R) primer sequence (5'-3')		Reference
ICER	NM_001110854.1	F:	5'TGAAACTGATGAGGAGACTGAC-3'	[21]
		R:	5'CAGCCATCACCACACCTTG-3'	
GAPDH	NM_001001303.1	F:	5'CAAGTTCAACGGCAGTCAAG-3'	[22]
		R:	5'ACATACTCAGCACCAGCATCAC-3'	

National Center for Biotechnology Information, US National Library of Medicine 8600 Rockville Pike, Bethesda, MD 20894, USA

S.E. Results were analyzed using one-way analysis of variance test (one-way ANOVA) followed by the least significant difference (LSD) criterion as a post-hoc test for comparing between different groups. The level of significance was fixed at $P \leq 0.05$ for all statistical tests.

Results

Liver function tests

All liver function tests (AST, ALT, GGT, and total and direct bilirubin) showed relatively constant values in the control rats during the 14 weeks follow-up periods; on the other hand, NAFLD rats showed duration-dependent increase. Compared to control rats, significantly higher levels of ALT, AST, GGT, total bilirubin, and direct bilirubin were observed in NAFLD rats as early as 2nd week of induction (Table 2). At the end of 14th week HFD induction, the NAFLD rats showed higher activities of ALT, AST, and GGT by about 3.45-, 4.32-, and 4.63-fold compared to control rats, respectively. In addition, total and direct bilirubin levels were higher to about 5.48- and 5.28-fold compared to that of control rats.

Lipid profile parameters

Serum lipid profile

The control rats demonstrated a relatively constant serum lipid profile during the follow-up period of 14 weeks with no significant changes during this period. Conversely, NAFLD rats showed typical duration-

dependent increase in serum lipid profile; TG, TC, and LDL-C and duration-dependent decline in the level of HDL-C. The results showed that NAFLD rats had significantly higher levels of serum TG, TC, and LDL-C compared to control rats as early as the 2nd week of induction. Moreover, NAFLD rats showed significant lower serum level of HDL-C compared to control rats from the 4th week of induction (Table 3). After 14 weeks of induction, NAFLD rats have significantly higher levels of serum TG, TC, and LDL-C, by about 1.92-, 2.03-, and 3.96-fold, compared to control values respectively, while HDL-C was lower than that of control value by about 2.73-fold.

Hepatic lipid content

In control rats, the hepatic TG content showed mild duration-dependent increase during the follow-up period while the hepatic TC content appeared to be relatively constant with no significant change during the study period. On the other hand, in NAFLD rats, the hepatic TG and TC contents showed significant duration-dependent elevation during 14 weeks of HFD feeding. The hepatic TG and TC contents were significantly higher in NAFLD rats compared to control rats as early as 2nd week of feeding (Table 3). At the end of 14 weeks of HFD feeding, NAFLD rats have higher level of hepatic TG and TC content by about 2.55- and 2.51-fold compared to control value, respectively.

Table 2 The liver function tests in serum of control and NAFLD groups

Weeks	ALT		AST		GGT		Total bilirubin		Direct bilirubin	
	Control	NAFLD	Control	NAFLD	Control	NAFLD	Control	NAFLD	Control	NAFLD
2	10.6 ± 1.29	18.6 ± 0.51*	12.2 ± 1.02	21.6 ± 1.21*	9.2 ± 0.73	16.8 ± 1.16*	0.59 ± 0.05	1.41 ± 0.05*	0.04 ± 0.02	0.18 ± 0.02*
4	12.0 ± 1.05	21.0 ± 1.38*#	13.8 ± 1.59	24.4 ± 1.54*#	10.4 ± 0.75	24.1 ± 2.32*#	0.58 ± 0.05	2.03 ± 0.06*#	0.07 ± 0.02	0.21 ± 0.01*
6	15.4 ± 1.57	28.6 ± 1.69*#	17.8 ± 1.39	39.4 ± 2.25*#	10.6 ± 1.40	34.4 ± 2.38*#	0.65 ± 0.06	2.65 ± 0.12*#	0.05 ± 0.02	0.22 ± 0.02*
8	13.6 ± 0.75	35.8 ± 1.93*#	17.0 ± 1.00	46.1 ± 1.79*#	11.8 ± 0.66	41.0 ± 1.95*#	0.67 ± 0.04	3.12 ± 0.23*#	0.07 ± 0.01	0.29 ± 0.02*
10	13.4 ± 1.03	40.8 ± 2.31*#	17.0 ± 1.76	53.8 ± 2.84*#	11.2 ± 0.84	46.0 ± 3.86*#	0.69 ± 0.05	3.60 ± 0.16*#	0.07 ± 0.02	0.34 ± 0.02*
12	15.6 ± 0.60	49.6 ± 2.11*#	16.8 ± 1.83	64.4 ± 3.30*#	12.2 ± 2.01	53.0 ± 4.37*#	0.71 ± 0.05	3.93 ± 0.05*#	0.10 ± 0.01	0.39 ± 0.02*
14	14.8 ± 1.62	60.6 ± 3.60*#	17.8 ± 1.5	85.4 ± 2.29*#	12.4 ± 0.51	62.6 ± 3.83*#	0.70 ± 0.02	4.28 ± 0.14*#	0.13 ± 0.01	0.44 ± 0.02*

Data expressed as mean ± SE

*Significant difference compared to control group at the same duration period by *t* test ($P < 0.05$)

#Significant difference compared to the previous duration in the same group by paired *t* test ($P < 0.05$)

Table 3 The serum lipid profile and hepatic lipid content of control and NAFLD groups

Weeks	Serum triglycerides level		Serum total cholesterol level		Serum LDL level		Serum HDL level		Hepatic triglyceride content		Hepatic cholesterol content	
	Control	NAFLD	Control	NAFLD	Control	NAFLD	Control	NAFLD	Control	NAFLD	Control	NAFLD
2	89.2 ± 3.83	221.4 ± 4.37*	76.4 ± 0.65	86.0 ± 2.90*	13.32 ± 1.01	39.12 ± 2.90*	45.74 ± 1.85	42.48 ± 1.57	41.2 ± 3.26	68.6 ± 6.68*	5.06 ± 7.51	85.0 ± 3.79*
4	102.7 ± 5.22	146.7 ± 6.55*#	76.0 ± 0.89	94.2 ± 2.63*	17.5 ± 2.25	56.90 ± 4.40*#	49.74 ± 1.66	37.04 ± 2.20*#	39.8 ± 2.75	81.6 ± 4.02*#	53.6 ± 8.16	98.0 ± 3.65*
6	108.6 ± 5.73	177.3 ± 8.39*#	81.0 ± 1.70	130.0 ± 2.86*#	24.22 ± 3.19	86.80 ± 6.44*#	48.68 ± 1.88	30.48 ± 1.58*#	42.6 ± 2.89	102.6 ± 3.72*#	52.2 ± 7.23	122.4 ± 4.59*#
8	95.1 ± 4.66	210.6 ± 10.71*#	85.8 ± 1.24	156.6 ± 4.40*#	29.96 ± 2.15	121.2 ± 3.23*#	49.6 ± 3.17	21.82 ± 1.80*#	41.0 ± 2.00	140.6 ± 4.69*#	58.6 ± 6.11	138.4 ± 5.97*#
10	106.2 ± 7.61	234.6 ± 8.62*#	91.8 ± 2.71	214.2 ± 5.28*#	32.18 ± 4.21	158.6 ± 4.94*#	51.52 ± 1.94	18.30 ± 1.77*#	44.8 ± 1.83	158.2 ± 4.86*#	62.8 ± 5.13	163.4 ± 5.80*#
12	109.7 ± 8.19	270.4 ± 10.6*#	98.2 ± 2.06	242.6 ± 3.83*#	31.40 ± 3.99	174.9 ± 3.79*#	51.86 ± 1.17	15.76 ± 1.42*#	50.4 ± 3.09	188.8 ± 2.62*#	65.6 ± 7.72	190.4 ± 5.47*#
14	111.5 ± 7.88	302.3 ± 11.47*#	108.2 ± 2.82	267.0 ± 2.07*#	37.48 ± 3.31	186.1 ± 4.28*#	51.02 ± 1.34	13.32 ± 1.55*#	57.2 ± 3.34	203.0 ± 4.57*#	69.2 ± 4.04	206.6 ± 4.25*#

Data expressed as mean ± SE

*Significant difference control group at the same duration period by t test ($P < 0.05$) compared to#Significant difference compared to the previous duration in the same group by paired t test ($P < 0.05$)

Glucose homeostasis parameters

All glucose homeostasis parameters in control rats showed relatively constant values for 14 weeks follow-up period. Conversely, the NAFLD rats showed a duration-dependent elevation of all parameters during 14 weeks of HFD feeding. Glucose level showed significant higher level in NAFLD group compared to control group from the 4th week of induction, and its level increased directly with the duration of induction. Hyperglycemia was detected at 10th week of induction and thereafter. Moreover, NAFLD rats showed significantly higher fasting insulin level than control rats as early as 4th week of induction. The calculation of insulin resistance index using HOMA-IRI showed that NAFLD rats had significantly higher degree of insulin resistance than that of control rats as early as 4th week of induction and thereafter (Table 4). At the end of 14 weeks of HFD feeding, the NAFLD rats showed significantly higher levels of fasting blood sugar, insulin, and HOMA-IRI by about 1.57-, 7.65-, and 24.64-fold compared to control values, respectively.

cAMP levels in liver tissue

The control rats showed relatively constant cAMP levels in the liver tissue during the follow-up period of 14 weeks with no significant changes during this period. In contrast, NAFLD rats showed typical duration-dependent increase in the cAMP levels in the liver. The results showed that NAFLD rats had significantly higher levels of cAMP in the liver compared to control rats from the 6th week of induction (Table 5). After 14 weeks of induction, NAFLD group has significantly higher levels of cAMP in the liver by about 3.79-fold that of control values.

CREB levels in liver tissue

No significant changes were observed in CREB levels in the liver tissue in control group during the follow-up period. On the other hand, NAFLD rats showed duration-dependent increase in CREB levels in the liver tissue. Compared to control rats, significantly

higher levels of CREB in the liver were observed in NAFLD rats from 6th week of induction (Table 5). At the end of 14 weeks of HFD feeding, the NAFLD group showed significantly higher levels of CREB in the liver tissue by about 8.01-fold that of control values.

Changes in gene expression of *ICER* in the liver tissues of control and NAFLD rats

The data of *ICER* gene expression relative to GAPDH was demonstrated in Fig. 1. The gene expression of *ICER* in the liver of control rats is almost constant during the follow-up period. In NAFLD rats, the gene expression of *ICER* in the liver showed duration-dependent decline. It was clear that the expression of *ICER* gene in the liver of NAFLD group was downregulated, but not significantly, compared to control group from 6th week of induction at which the expression in the liver was about 88% of the control value. The expression at 14th week of induction showed duration-dependent downregulation to reach 18% of control value.

Correlation studies

In NAFLD rats, the statistical analysis using Spearman correlation was revealed that there was a direct positive correlation between cAMP and CREB levels, while level of *ICER* gene expression was negatively correlated with cAMP and CREB levels as in Fig. 2. In addition, CREB levels were positively correlated with liver function tests, fasting glucose level, fasting insulin level, HOMA-IR, and with all lipid profile parameters, except HDL-cholesterol which was negatively correlated with CREB.

Histological assessment

The hepatic lesions in NAFLD were divided into three main categories: nonalcoholic fatty liver (NAFL), nonalcoholic steatohepatitis (NASH), and cirrhosis. Areas of overlap exist between these three main patterns of liver injury,

Table 4 The glucose homeostasis parameters of control and NAFLD groups

Weeks	Fasting glucose		Fasting insulin level		Insulin resistance	
	Control	NAFLD	Control	NAFLD	Control	NAFLD
2	73.2 ± 2.18	81.8 ± 3.07	0.70 ± 0.13	1.15 ± 0.23	0.12 ± 0.03	0.23 ± 0.04
4	72.4 ± 3.41	89.8 ± 3.35*#	0.90 ± 0.14	2.67 ± 0.16*#	0.15 ± 0.03	0.58 ± 0.02*#
6	77.2 ± 4.35	104.4 ± 5.15*#	0.95 ± 0.16	3.40 ± 0.20*#	0.17 ± 0.02	0.87 ± 0.02*#
8	74.8 ± 3.34	118.6 ± 4.08*#	0.86 ± 0.17	4.50 ± 0.39*#	0.15 ± 0.03	1.28 ± 0.06*#
10	76.6 ± 3.61	137.8 ± 3.56*#	0.76 ± 0.18	5.52 ± 0.38*#	0.14 ± 0.03	1.82 ± 0.07*#
12	80.4 ± 4.66	167.0 ± 3.26*#	0.90 ± 0.14	6.74 ± 0.39*#	0.17 ± 0.02	2.74 ± 0.12*#
14	80.6 ± 3.67	196.4 ± 5.81*#	0.94 ± 0.13	8.13 ± 0.37*#	0.18 ± 0.02	3.95 ± 0.11*#

Data expressed as mean ± SE

*Significant difference compared to control group at the same duration period by *t* test ($P < 0.05$)

Significant difference compared to the previous duration in the same group by paired *t* test ($P < 0.05$)

Table 5 The liver tissue cAMP and CREB levels in control and NAFLD rats

Weeks	cAMP level (pg/mg liver protein)		CREB level (ng/mg liver protein)	
	Control	NAFLD	Control	NAFLD
2	4.08 ± 0.64	4.03 ± 1.16	0.76 ± 0.18	0.90 ± 0.20
4	3.59 ± 0.86	5.69 ± 0.74*#	0.84 ± 0.14	1.87 ± 0.36
6	4.20 ± 0.91	7.81 ± 2.05*#	0.75 ± 0.15	3.21 ± 0.72*#
8	3.95 ± 0.85	8.30 ± 1.13*#	0.95 ± 0.06	4.47 ± 0.80*#
10	4.65 ± 0.42	11.93 ± 1.83*#	0.88 ± 0.19	5.49 ± 0.62*#
12	3.91 ± 0.90	15.31 ± 1.51*#	0.79 ± 0.17	6.35 ± 0.63*#
14	4.25 ± 0.86	19.61 ± 1.63*#	0.82 ± 0.16	7.44 ± 0.59*#

Data expressed as mean ± SE

*Significant difference compared to control group at the same duration period by *t* test (*P* < 0.05)

#Significant difference compared to the previous duration in the same group by paired *t* test (*P* < 0.05)

and they are probably best regarded as different parts of a broad histological spectrum (Fig. 3).

Histological examination of the livers from NAFLD rats demonstrated the progressive development of substantial steatosis with inflammatory changes throughout the study periods.

Phosphorylated CREB (phosphor-S133) visualization by immunofluorescence

pCREB immunofluorescence was slightly detected in the control rats, with 1.7 ± 0.5 MA% and 2188.07 ± 446.04 fluorescence intensity. After 6 weeks of HFD induction, the intensity of immunofluorescence signal as well as its MA% increased significantly in NAFLD rats to record 142.3-fold increase (*P* < 0.04) and 13.6 ± 1.7 (*P* < 0.005),

respectively. Similar significant increases were observed at the 10th week, where intensity of cell fluorescence increased by 158.9-fold and MA% recorded 35.2 ± 0.8 (*P* < 0.0001). Interestingly, both pCREB immunofluorescence signal and MA% showed duration-dependent increase in NAFLD rats to become more prominent at the end of the experiment (14th week), Fig. 4.

Discussion

Nonalcoholic fatty liver disease (NAFLD) has become the most common chronic liver with hepatocellular lipid deposition followed by inflammation. NAFLD has been considered as hepatic manifestation of metabolic syndrome and consists of progressive stages, ranging from simple steatosis to NASH, fibrosis, and cirrhosis. In the

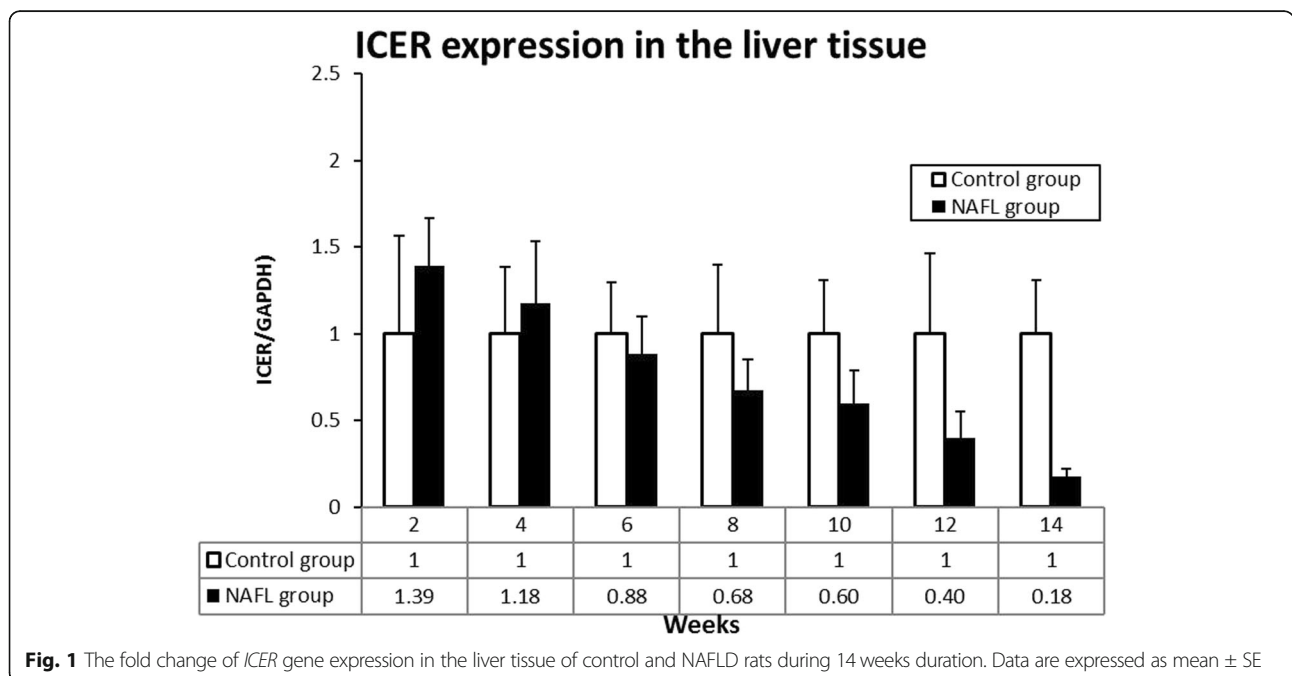
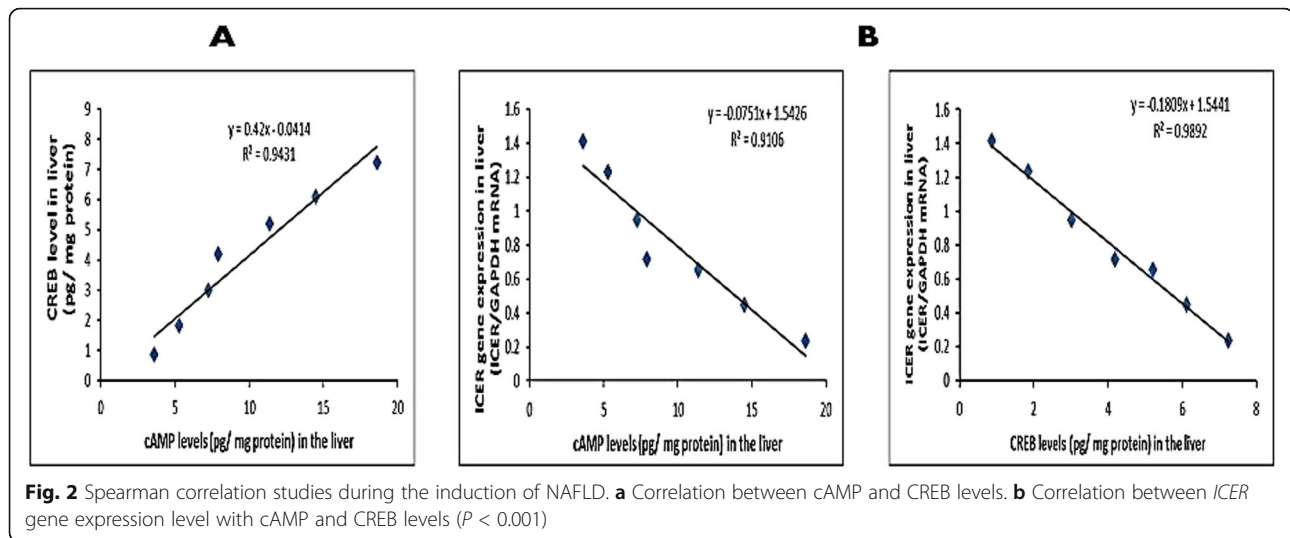


Fig. 1 The fold change of *ICER* gene expression in the liver tissue of control and NAFLD rats during 14 weeks duration. Data are expressed as mean ± SE



patients with a sedentary lifestyle, obesity, or IR, an increased influx of free fatty acid (FFA) to the hepatocyte was observed in the liver. While several factors, such as obesity, diabetes, and dyslipidemia, have been implicated in NAFLD, the pathogenesis of NAFLD and its progression to fibrosis and chronic liver disease are still unclear [26].

It has been proposed that NAFLD may be considered as a disease with a “two-hit” process of pathogenesis with lipid peroxidation-mediated liver injury. The “first hit” is excessive hepatocyte triglyceride accumulation which may result from insulin resistance. The second hit is unclear, but the presumed factors initiating second hits are suggested to be oxidative stress and subsequent lipid peroxidation and proinflammatory cytokines [27].

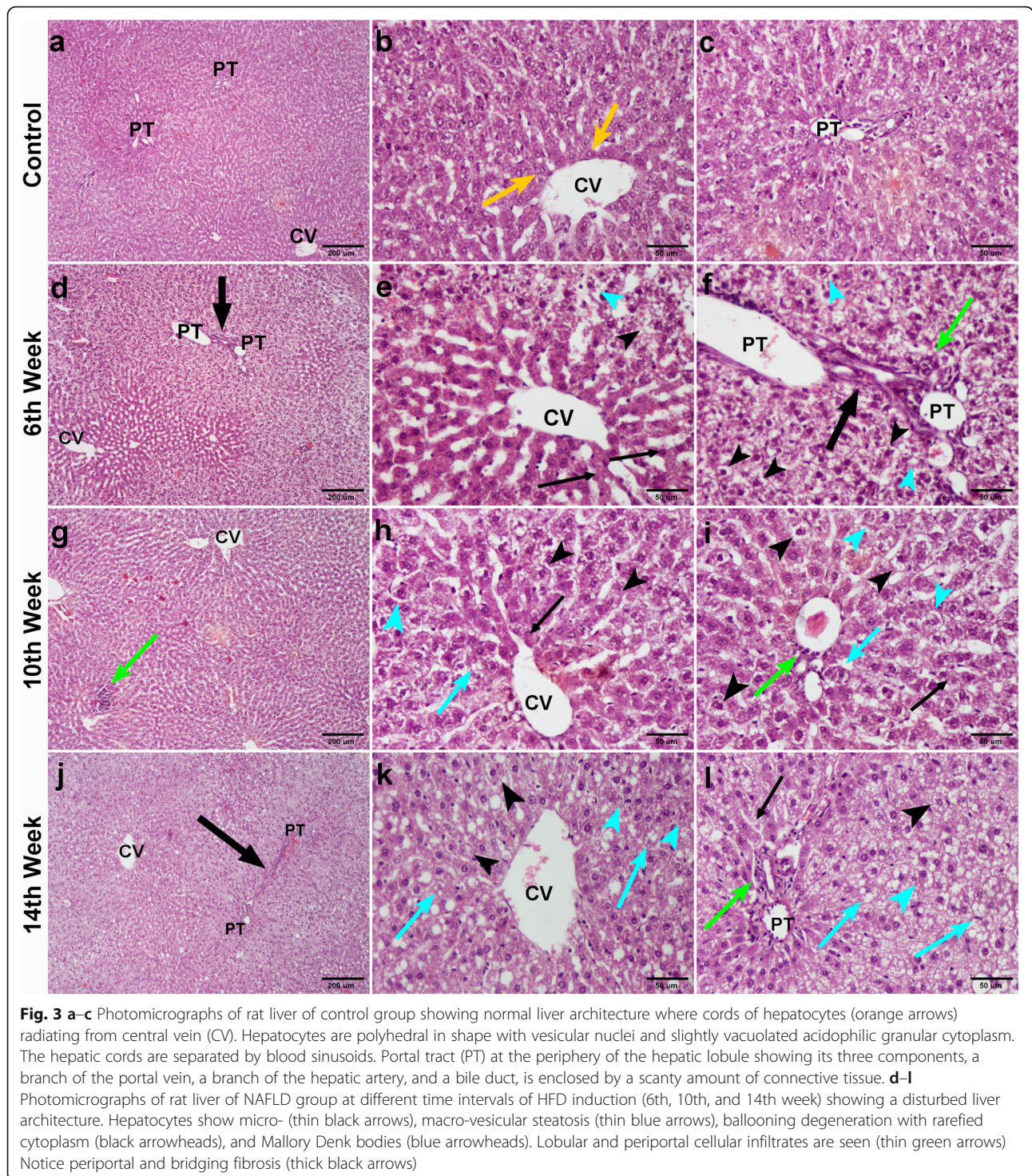
Several data supported the implication of cAMP response element-binding protein (CREB) in NAFLD progress. The aim of this study is to evaluate the role of hepatic cAMP/CREB pathway in the development of experimental nonalcoholic fatty liver to clarify its pathogenesis which could provide a therapeutic approach. In our study, we used a HFD rat model of insulin resistance and NASH because it is easy to establish and resemble the human condition.

Histological examination of the liver tissues in control group revealed better liver histology, with normal hepatic architecture and organization, when compared to NAFLD one. Few hepatocytes showed rarefaction of the cytoplasm and micro-vesicular steatosis at 6th week of HFD induction. At 10th week of feeding, hepatocytes showed rarefied cytoplasm with micro- and macro-vesicular steatosis and hepatocellular ballooning. Mallory’s bodies, hyaline eosinophilic irregular-shaped aggregates in the cytoplasm of hepatocytes, were also present. The liver tissues of the NAFLD group at 14th week of HFD induction demonstrated more disturbance of the hepatic architecture;

marked Mallory’s bodies, macro-vesicular steatosis, periportal inflammatory cellular infiltrates, and bridging fibrosis were noticed. The majority of authors on this topic consider the presence of fat, ballooning, and hepatocyte injury to be the minimum histopathological changes required for establishing a diagnosis of NASH which evolves into advanced fibrosis [28]. In accordance with our results, Lieber et al., who used the quietly similar type of high-fat diet for only 3 weeks in Sprague-Dawley rats, reproduced hepatic lesions of human NASH [29]. Moreover, another study demonstrated that Wistar rats seem to be more sensitive to developing steatosis when consuming diets with a higher fat content in comparison with Sprague-Dawley rats [30].

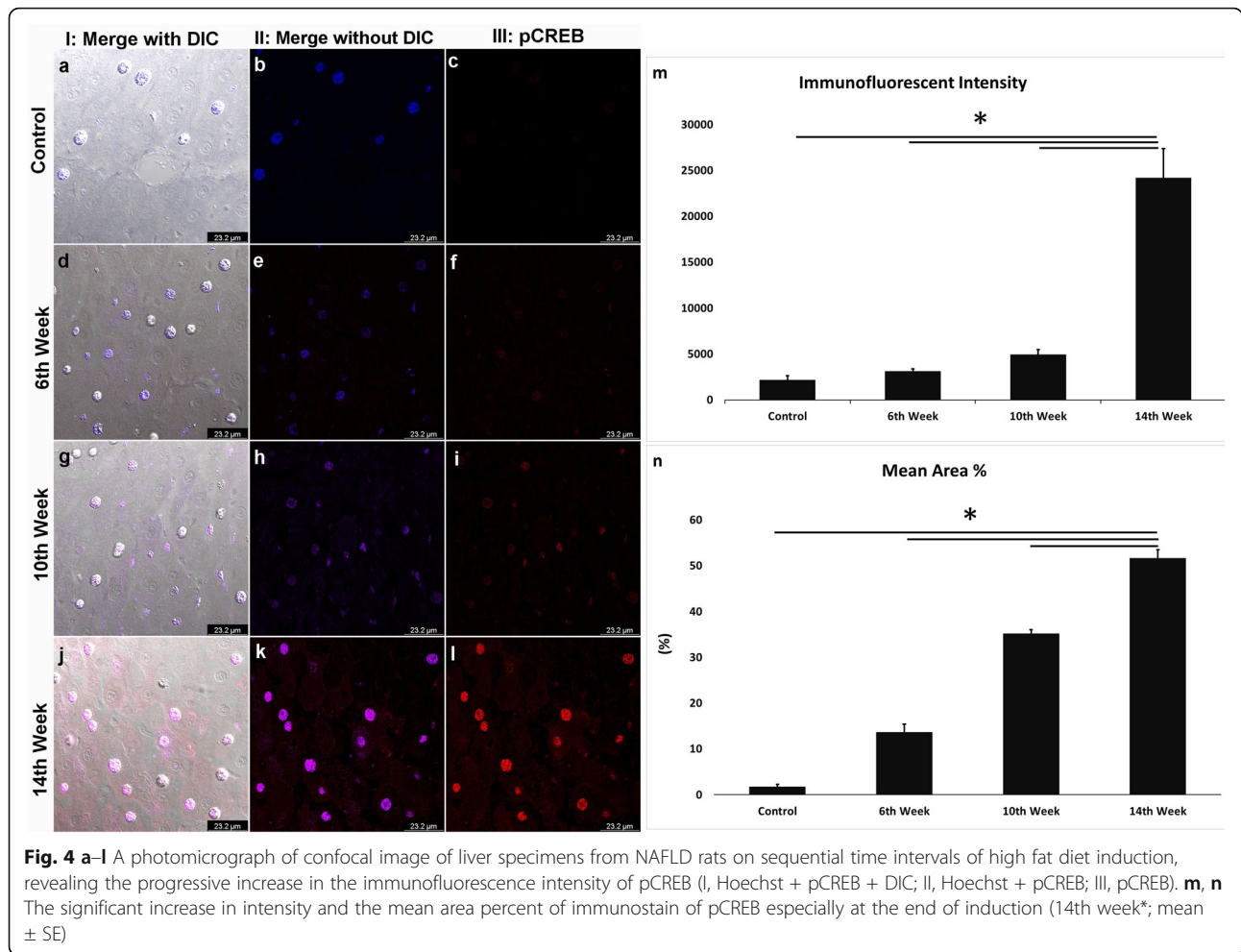
The AST, ALT, GGT, and levels of total and direct bilirubin among other markers of liver injury may be useful parameters in measuring NAFLD. The results of the present study revealed a remarkable increase in these parameters in NAFLD rats as early as 2nd week of induction compared to control group. Our results are in accordance with those reported by Hanafi et al., who showed that the activities of serum transaminases, AST, ALT, and GGT, were significantly increased in NAFLD rats. Also, NAFLD rats demonstrated higher bilirubin values [31]. These significant abnormalities of liver function tests revealed a state of hepatocytes inflammation and slightly damage as indicated by the histological results.

In the current work, dyslipidemia was evidenced in the NAFLD group from the second week of HFD as indicated by a significant increase in triglycerides, cholesterol, and LDL-cholesterol levels. Moreover, HDL-cholesterol was significantly decreased in the NAFLD group from the 4th week of induction. Hypertriglyceridemia and abnormal low level of HDL-cholesterol are evidenced in the course of induction



from the 6th week of feeding while hypercholesterolemia and abnormal high level of LDL-cholesterol are detected later at the 10th week. Moreover, NAFLD rats revealed typical duration–dependent increase in serum lipid profile including TG, TC, and LDL-C and duration-dependent decline in the level of HDL-C. In agreement with these results, it was reported that dyslipidemias are

common abnormalities observed in NAFLD and have been reported in up to 81% of patients [32]. It is suggested that hyper-triglyceridemia is more likely to increase the risk of NAFLD than hypercholesterolemia [33, 34]. Furthermore, many evidences suggest that among different types of cholesterol, abnormality of HDL-C is the most frequent lipid profile in NASH



patients, while LDL-C as well as total cholesterol are more likely to be within normal ranges [35].

An increase in intrahepatic fat content leads to an up-regulation of oxidative mechanisms, or it can be re-esterified and secreted again as hepatic VLDL-triglycerides (TG), the major source of circulating TG [36, 37], which is responsible for the increase in serum TG concentrations observed in our study. However, the liver capacity in NAFLD to export TG is limited by an inadequate increase of the secretion rate of apoB100. A reduction in apo B synthesis and secretion may impair hepatic lipid export and favor hepatic triglyceride accumulation [38], which was confirmed in histopathological assessment of our study from the 2nd week of NAFLD induction. The current work revealed a significant raise in the hepatic TG and TC content in the liver of the NAFLD group compared to control rats as early as 2nd week of feeding. Additionally, there was a significant duration-dependent elevation in the hepatic TG and TC liver contents in the NAFLD rats during 14 weeks of HFD feeding.

One of our promising findings is that hepatic TG accumulation proceeds or at least concomitant with hyperinsulinemia at 4th week and IR which also became significant from the 4th week of induction. In accordance with these results, it was reported that once the liver is fatty, the ability of insulin to inhibit hepatic glucose production is impaired, which leads to an increase in the fasting plasma glucose concentration [39]. This in turn stimulates insulin secretion resulting in mild hyperinsulinemia and lowering of glucose to near-normal levels; also, the inhibitory action of insulin on VLDL production is impaired whereas VLDL clearance remains unchanged [40, 41].

The association between IR and NAFLD is an area of public health impact. IR and subsequent compensatory hyperinsulinemia have been shown to have a key role in the pathogenesis of NAFLD by causing an imbalance between factors that favor hepatic lipid accumulation (such as lipid influx and de novo lipid synthesis) and factors that ameliorate lipid build-up, such as lipid export or oxidation [42, 43].

Abnormally elevated insulin levels, under IR conditions, are required to metabolize glucose and inhibit hepatic glucose production effectively due to the reduced insulin sensitivity of the peripheral tissues. In this context, the pancreas is stimulated to increase insulin secretion into the portal vein, leading to higher insulin levels in the liver than in the periphery. High concentrations of hepatic glucose and plasma insulin are recognized as biomarkers of hepatic IR [44]. Elevated fasting glucose results from hepatic IR, whereas increased FFA concentrations are caused by peripheral IR. The FFAs interact with insulin signaling, thereby contributing to IR. Hepatic IR contributes to steatosis of NAFLD by impairing insulin receptor substrate 1/2 tyrosine phosphorylation [45, 46].

As expected in our results, during NAFLD induction, a fasting glucose level is significantly higher in NAFLD group compared to control group from the 2nd week of induction, and its level increased directly with the duration of induction. Hyperglycemia was detected at 10th week of induction and thereafter. Also, fasting insulin and insulin resistance index (HOMA-IR) revealed higher degrees of IR from the 4th week of induction, and with increasing duration, the situation become worse. Furthermore, these abnormalities of glucose homeostasis during HFD feeding are associated with serious derangements in lipid profile as discussed previously.

The cAMP is a key second messenger in numerous signal transduction pathways including cell growth, differentiation, gene transcription, protein expression, and in the regulation of cellular metabolism as well as hormonal action in the peripheral tissues. Subsequently, specific proteins are phosphorylated by PKA to evoke cellular reactions. The phosphorylation of CREB, a transcription factor, is important in the regulation of gene transcription. Extracellular signals activate the transcription of a variety of target genes via alterations in CREB phosphorylation, thereby, resulting in multiple physiological functions [47, 48].

CREB activity is tightly regulated by phosphorylation as well as by the level of ICER, a natural CREB antagonist. ICER is generated from an alternative CREM promoter and is the only inducible CRE-binding protein. ICER acts as a passive repressor that competes with CREB for binding to target gene promoters. In the normal situation, ICER activity is transiently induced by the same stimuli that induce CREB, but repression occurs only when ICER reaches certain levels [49, 50]. There is a strong evidence for the association between CREB and ICER, while CREB rapidly induces the expression of target genes in response to stimuli; the repressor ICER restores their initial expression levels and thereby permits transient induction [51].

Stimuli that trigger CREB and ICER activities include cell proliferation, cell cycle, metabolism, DNA repair, differentiation, inflammation, angiogenesis, immune responses, and survival response for instance, and this occurs in response to an elevation of cAMP levels. Thereby, as a passive repressor, ICER activity is directly correlated with its abundance [49, 52]. It is thus predictable that dysregulation in the levels of ICER impact to CREB activity, hence leading to cells dysfunction and eventually certain pathologies.

Our results indicated that, in NAFLD rats, the hepatic contents of cAMP and CREB are prominently elevated compared to control rats. Furthermore, the results showed that NAFLD rats feeding HFD revealed a typical duration-dependent increase in both cAMP and CREB levels in the liver tissue. Notably, the results of the present study also demonstrated that the expression of *ICER* gene in the liver tissue was downregulated in NAFLD rats from 6th week of induction compared to control rats. This is in close agreement with the results of Favre et al. who found that the expression of *ICER* was decreased in insulin-resistant obese mice indicating an impaired induction of *ICER* and, hence, leading to persistently increased CREB activity [53].

The significant high level of both cAMP and CREB levels in the liver could be explained by IR state, a prominent factor of NAFLD, which favors the lipolytic pathway as a consequence of increasing glucagon/insulin ratio; the generated FFAs and glycerol may further exaggerate the IR in tissues in a vicious cycle. Our study is in accordance with Erion et al. findings who used a CREB-specific antisense oligonucleotide (ASO) to knock down CREB expression in the liver. Interestingly, CREB ASO treatment dramatically reduced fasting plasma glucose concentrations in Zucker Diabetic Fatty rats and a streptozotocin-treated high-fat fed rat model of type II diabetes mellitus (T2DM) with its concomitant IR [54]. Nonetheless, our results are not in accordance with the study of Zingg et al. who reported that, in the liver, the HFD significantly decreased liver cAMP levels compared to low fat diet, and curcumin increased it [55]. Furthermore, a study investigating the therapeutic effects of resveratrol, a naturally occurring polyphenol, in NAFLD showed that its protective effects were mediated by the cAMP pathway. In particular, resveratrol improved hepatic steatosis in a HFD mouse model of NAFLD via improved fatty acid β -oxidation by increasing cAMP through inhibiting PDE4 [56].

Correlation studies revealed a direct positive correlation between the intracellular level of cAMP and CREB in the liver tissue. On the other hand, the levels of cAMP and CREB in the liver tissue were negatively correlated with the *ICER* gene expression. Moreover, the level of cAMP in the liver tissue was positively correlated

with fasting blood glucose, insulin, HOMA, liver function tests (ALT, AST, GGT, total bilirubin, direct bilirubin), lipid profile tests (serum triglycerides, cholesterol, LDL-cholesterol, but not HDL-cholesterol) as well as hepatic triglycerides and cholesterol contents. Contrariwise, the level of cAMP was negatively correlated with the level of HDL-cholesterol.

Conclusions

Finally, from the discussion of the present study and other studies, we can conclude that the persistent elevation of intracellular cAMP levels, and consequently dysregulation of its signaling pathways, play an important role in the induction of NAFLD by HFD. However, the order of events and the interrelationships between different pathways in the development of NAFLD need further investigation in order to find suitable interventions for the design of novel therapeutic strategies. Moreover, considering the implication of downstream cAMP pathway in the pathogenesis on NAFLD, further investigation of the interplay between CREB activity and ICER expression may reveal drug targets for treatment of the disease.

Abbreviations

ALT: Alanine aminotransferase; ASO: CREB-specific antisense oligonucleotide; AST: Aspartate aminotransferase; cAMP: Cyclic adenosine monophosphate; CRE: cAMP-response elements; CREB: cAMP response element-binding protein; CREM: cAMP response element-modulator; FFA: Free fatty acid; GAPDH: Glyceraldehyde 3-phosphate dehydrogenase; GGT: Gamma glutamyl transferase; HDL-C: High-density lipoprotein cholesterol; HFD: High fat diet; HOMA-IR: Homeostatic model assessment of insulin resistance; ICER: Inducible cAMP early repressor; IR: Insulin resistance; IRI: Insulin resistance index; LDL-C: Low-density lipoprotein cholesterol; MA%: Mean area percent; NAFL: Nonalcoholic fatty liver; NAFLD: Nonalcoholic fatty liver disease; NASH: Nonalcoholic steatohepatitis; pCREB: Phosphorylated CREB; PKA: Protein kinase A; RT-PCR: Reverse transcriptase polymerase chain reaction; TC: Total cholesterol; TG: Triglycerides; VLDL: Very low-density lipoprotein

Acknowledgements

We express our deep gratitude to the staff members in the Center of Excellence for Research in Regenerative Medicine and Applications (CERRMA; a STDF-funded Center of Excellence), Faculty of Medicine, Alexandria University, Egypt, for providing their support in completion of the study, with especial thanks to Prof. Ghada Mourad the executive manager of the Medical Research Center for facilitating the use of the confocal imaging unit.

Authors' contributions

AA collected, analyzed, and interpreted the biochemical and confocal data and was the major contributor in writing the manuscript. MK helped in the conceptualization and designing of the study. MH and MH helped in the interpretation of the biochemical data. MM helped in the interpretation of the biochemical data and editing the manuscript. MY and EZ performed the histological examination of the liver tissue. ME performed the examination and morphometric analysis of the confocal images and contributed in manuscript editing. All authors read and approved the final manuscript

Funding

Not applicable. The study was fully non-funded from any organization.

Availability of data and materials

All data generated or analyzed during this study are included in this published article.

Ethics approval and consent to participate

Alexandria University Institutional Animal Care and Use Committee (ALEXUIACUC; AU01220051022) has approved the current animal study, and the procedures followed are in accordance with institutional guidelines.

Consent for publication

Not applicable.

Competing interests

The authors declare that they have no competing interests.

Author details

¹Biochemistry Department, Faculty of Science, Ain Shams University, Cairo, Egypt. ²Biochemistry Department, Medical Research Institute, Alexandria University, Alexandria, Egypt. ³Center of Excellence for Research in Regenerative Medicine and Applications (CERRMA), Faculty of Medicine, Alexandria University, Alexandria, Egypt. ⁴Histochemistry and Cell Biology Department, Medical Research Institute, Alexandria University, Alexandria, Egypt. ⁵Histology and Cell Biology Department, Faculty of Medicine, Alexandria University, Alexandria, Egypt. ⁶Oral Pathology Department, Faculty of Dentistry, Alexandria University, Alexandria, Egypt.

Received: 6 May 2020 Accepted: 17 July 2020

Published online: 28 July 2020

References

- Mantovani A, Scorletti E, Mosca A, Alisi A, Byrne CD, Targher G (2020) Complications, morbidity and mortality of nonalcoholic fatty liver disease. *Metabolism*:154170
- Negro F (2020) Natural history of NASH and HCC. *Liver Int* 40:72–76
- Malnick S, Maor Y (2020) The interplay between alcoholic liver disease, obesity, and the metabolic syndrome. *Visceral Medicine*:1–8
- Severson TJ, Besur S, Bonkovsky HL (2016) Genetic factors that affect nonalcoholic fatty liver disease: a systematic clinical review. *World J Gastroenterol* 22:6742
- Fabbri E, Sullivan S, Klein S (2010) Obesity and nonalcoholic fatty liver disease: biochemical, metabolic, and clinical implications. *Hepatology* 51: 679–689
- Khannpnavar B, Mehta V, Qi C, Korkhov V (2020) Structure and function of adenylyl cyclases, key enzymes in cellular signaling. *Curr Opin Struct Biol* 63: 34–41
- Naqvi S, Martin KJ, Arthur JSC (2014) CREB phosphorylation at Ser133 regulates transcription via distinct mechanisms downstream of cAMP and MAPK signalling. *Biochem J* 458:469–479
- Favre D, Le Gouill E, Fahmi D et al (2011a) Impaired expression of the inducible cAMP early repressor accounts for sustained adipose CREB activity in obesity. *Diabetes* 60:3169–3174
- Zmrzljak UP, Korenčič A, Goličnik M, Sassone-Corsi P, Rozman D (2013b) Inducible cAMP early repressor regulates the Period 1 gene of the hepatic and adrenal clocks. *J Biol Chem* 288:10318–10327
- Han H-S, Kang G, Kim JS, Choi BH, Koo S-H (2016) Regulation of glucose metabolism from a liver-centric perspective. *Exp Mol Med* 48:e218
- Wang Y, Viscarra J, Kim S-J, Sul HS (2015) Transcriptional regulation of hepatic lipogenesis. *Nat Rev Mol Cell Biol* 16:678
- Petersen MC, Vatner DF, Shulman GI (2017) Regulation of hepatic glucose metabolism in health and disease. *Nat Rev Endocrinol* 13:572
- Rui L (2011) Energy metabolism in the liver. *Comprehensive physiology* 4: 177–197
- Shawky HA, Essawy MM (2018) Effect of atorvastatin and remifemin on glucocorticoid induced osteoporosis in rats with experimental periodontitis. A comparative study. *Egyptian Dental Journal* 64:2287–2296
- Estadella D, Oyama LM, Dâmaso AR, Ribeiro EB, Do Nascimento CMO (2004) Effect of palatable hyperlipidic diet on lipid metabolism of sedentary and exercised rats. *Nutrition* 20:218–224
- Folch J, Lees M, Sloane Stanley G (1957) A simple method for the isolation and purification of total lipides from animal tissues. *J Biol Chem* 226:497–509
- Matthews D, Hosker J, Rudenski A, Naylor B, Treacher D, Turner R (1985) Homeostasis model assessment: insulin resistance and β -cell function from fasting plasma glucose and insulin concentrations in man. *Diabetologia* 28: 412–419

18. Serezani CH, Ballinger MN, Aronoff DM, Peters-Golden M (2008) Cyclic AMP: master regulator of innate immune cell function. *Am J Respir Cell Mol Biol* 39:127–132
19. Lowry OH, Rosebrough NJ, Farr AL, Randall RJ (1951) Protein measurement with the Folin phenol reagent. *J Biol Chem* 193:265–275
20. Livak KJ, Schmittgen TD (2001) Analysis of relative gene expression data using real-time quantitative PCR and the 2⁻ $\Delta\Delta$ CT method. *Methods* 25: 402–408
21. Zmrzljak UP, Korencic A, Golicnik M, Sassone-Corsi P, Rozman D (2013a) Inducible cAMP early repressor regulates Period 1 gene of the hepatic and adrenal clocks. *Journal of Biological Chemistry* jbc. M112. 445692
22. Kim I, Yang D, Tang X, Carroll JL (2011) Reference gene validation for qPCR in rat carotid body during postnatal development. *BMC research notes* 4: 440
23. Bancroft JD, Gamble M (2008) Theory and practice of histological techniques. Elsevier health sciences,
24. Carleton H, Drury R, Wallington E (1980) Carleton's histological technique: Oxford University Press, USA,
25. Bártová E, Večeřa J, Krejčí J, Legátová S, Pacherník J, Kozubek S (2016) The level and distribution pattern of HP1 β in the embryonic brain correspond to those of H3K9me1/me2 but not of H3K9me3. *Histochem Cell Biol* 145: 447–461
26. Rosso N, Bellentani S (2020) Nonalcoholic fatty liver disease: a wide spectrum disease. In: *Liver diseases*. Springer, pp 273–284
27. Fang Y-L, Chen H, Wang C-L, Liang L (2018) Pathogenesis of non-alcoholic fatty liver disease in children and adolescence: from “two hit theory” to “multiple hit model”. *World J Gastroenterol* 24:2974
28. Brown GT, Kleiner DE (2016) Histopathology of nonalcoholic fatty liver disease and nonalcoholic steatohepatitis. *Metabolism* 65:1080–1086
29. Lieber CS, Leo MA, Mak KM et al (2004) Model of nonalcoholic steatohepatitis. *Am J Clin Nutr* 79:502–509. <https://doi.org/10.1093/ajcn/79.3.502>
30. London RM, George J (2007) Pathogenesis of NASH: animal models. *Clinics in liver disease* 11:55–74
31. Hanafi MY, Zaher EL, El-Adely SE et al (2018) The therapeutic effects of bee venom on some metabolic and antioxidant parameters associated with HFD-induced non-alcoholic fatty liver in rats. *Experimental and therapeutic medicine* 15:5091–5099
32. Tsochatzis E, Papatheodoridis G, Manesis E, Kafiri G, Tiniakos D, Archimandritis A (2008) Metabolic syndrome is associated with severe fibrosis in chronic viral hepatitis and non-alcoholic steatohepatitis. *Aliment Pharmacol Ther* 27:80–89
33. Ali S (2006) *Liver Diseases (2 Vols.): Biochemical mechanisms and new therapeutic insights*. CRC Press,
34. Saltzman E (2013) *Gastrointestinal and Liver Disease Nutrition Desk Reference*. Gastroenterology 145:250
35. Du T, Sun X, Yu X (2017) Non-HDL cholesterol and LDL cholesterol in the dyslipidemic classification in patients with nonalcoholic fatty liver disease. *Lipids Health Dis* 16:229
36. Alves-Bezerra M, Cohen DE (2011) Triglyceride metabolism in the liver. *Comprehensive Physiology* 8:1–22
37. Donnelly KL, Smith CI, Schwarzenberg SJ, Jessurun J, Boldt MD, Parks EJ (2005) Sources of fatty acids stored in liver and secreted via lipoproteins in patients with nonalcoholic fatty liver disease. *J Clin Invest* 115:1343–1351
38. Perla F, Prelati M, Lavorato M, Visicchio D, Anania C (2017) The role of lipid and lipoprotein metabolism in non-alcoholic fatty liver disease. *Children* 4:46
39. Girard J (2006) The inhibitory effects of insulin on hepatic glucose production are both direct and indirect. *Diabetes* 55:565–569
40. Adeli K, Lewis GF (2008) Intestinal lipoprotein overproduction in insulin-resistant states. *Curr Opin Lipidol* 19:221–228
41. Ginsberg HN, Zhang Y-L, Hernandez-Ono A (2005) Regulation of plasma triglycerides in insulin resistance and diabetes. *Arch Med Res* 36:232–240
42. Chen Z, Yu R, Xiong Y, Du F, Zhu S (2017) A vicious circle between insulin resistance and inflammation in nonalcoholic fatty liver disease. *Lipids Health Dis* 16:203
43. Kitade H, Chen G, Ni Y, Ota T (2017) Nonalcoholic fatty liver disease and insulin resistance: new insights and potential new treatments. *Nutrients* 9:387
44. Fujii H, Kawada N, NAFLD JSGo (2020) The role of insulin resistance and diabetes in nonalcoholic fatty liver disease. *Int J Mol Sci* 21:3863
45. Mu W, Cheng X-F, Liu Y, Lv Q-Z, Liu G-L, Zhang J-G, Li X-Y (2019) Potential nexus of non-alcoholic fatty liver disease and type 2 diabetes mellitus: insulin resistance between hepatic and peripheral tissues. *Front Pharmacol* 9:1566
46. Petersen MC, Samuel VT, Petersen KF, Shulman GI (2020) Non-alcoholic fatty liver disease and insulin resistance. *The Liver: Biology and Pathobiology*:455–471
47. Wahlang B, McClain C, Barve S, Gobejishvili L (2018) Role of cAMP and phosphodiesterase signaling in liver health and disease. *Cell Signal* 49:105–115
48. Wang H, Xu J, Lazarovici P, Quirion R, Zheng W (2018) cAMP response element-binding protein (CREB): a possible signaling molecule link in the pathophysiology of schizophrenia. *Front Mol Neurosci* 11:255
49. Dufour J-F, Clavien P-A, Graf R, Trautwein C (2010) Signaling pathways in liver diseases. Springer,
50. Lv S, Li J, Qiu X, Li W, Zhang C, Zhang Z-N, Luan B (2017) A negative feedback loop of ICER and NF- κ B regulates TLR signaling in innate immune responses. *Cell Death Differ* 24:492–499
51. Han W, Takamatsu Y, Yamamoto H et al. (2011) Inhibitory role of inducible cAMP early repressor (ICER) in methamphetamine-induced locomotor sensitization. *PLoS one* 6
52. Steven A, Seliger B (2016) Control of CREB expression in tumors: from molecular mechanisms and signal transduction pathways to therapeutic target. *Oncotarget* 7:35454
53. Favre D, Niederhauser G, Fahmi D et al (2011b) Role for inducible cAMP early repressor in promoting pancreatic beta cell dysfunction evoked by oxidative stress in human and rat islets. *Diabetologia* 54:2337–2346
54. Erion DM, Ignatova ID, Yonemitsu S et al (2009) Prevention of hepatic steatosis and hepatic insulin resistance by knockdown of cAMP response element-binding protein. *Cell Metab* 10:499–506
55. Zingg JM, Hasan ST, Nakagawa K et al (2017) Modulation of cAMP levels by high-fat diet and curcumin and regulatory effects on CD36/FAT scavenger receptor/fatty acids transporter gene expression. *Biofactors* 43:42–53
56. Zhang Y, Chen ML, Zhou Y et al (2015) Resveratrol improves hepatic steatosis by inducing autophagy through the cAMP signaling pathway. *Mol Nutr Food Res* 59:1443–1457

Publisher's Note

Springer Nature remains neutral with regard to jurisdictional claims in published maps and institutional affiliations.

Submit your manuscript to a SpringerOpen[®] journal and benefit from:

- Convenient online submission
- Rigorous peer review
- Open access: articles freely available online
- High visibility within the field
- Retaining the copyright to your article

Submit your next manuscript at ► [springeropen.com](https://www.springeropen.com)